J. Fluid Mech. (1966), *vol.* 24, *part* 1, *pp.* 177–189
Printed in Great Britain

The steady state exothermal hydromagnetic discontinuity for an arbitrarily orientated magnetic field

By LAWRENCE A. KENNEDY*
Department of Mechanical Engineering and Astronautical Sciences,
Northwestern University, Evanston, Illinois

(Received 23 April 1965)

An exothermal hydromagnetic discontinuity in a perfectly conducting gas is studied for the case of an arbitrarily orientated magnetic field. The evolutionary modes and the manner of variation of the physical properties for such phenomena are determined. The Hugoniot adiabatic is obtained and analysed.

1. Introduction

While the phenomenon of MHD shock discontinuities has been extensively investigated, the study of exothermal hydromagnetic discontinuities has scarcely been touched. In the near future, it is expected that this latter phenomenon will be of importance in controlled nuclear fusion devices, where a large energy release may occur in a hydromagnetic wave under the influence of a magnetic field. Also stellar phenomena, such as the propagation of detonation waves from the interior to the surface of a star accompanied by a release of nuclear energy on the wave-front, will be described by exothermal hydromagnetic waves.

Larish & Skekhtmann (1958) initially studied this phenomenon for the special case where the magnetic field was parallel to the discontinuity surface and the flow velocity was normal to it. Lyubimov (1959) further considered this problem in his studies of the velocity of the gas at the singular solution for both the magnetic and classical cases. This same problem was also investigated numerically by Gross, Chinitz & Rivlin (1960) and by Fong, Bollinger & Edse (1961). More recently Helliwell (1962) has reformulated this case, repeating the earlier work and attempting to take into account a jump in the electrical conductivity of the gas across the discontinuity.

Demutskii & Polovin (1961) have studied exothermic and endothermic discontinuities for the general magneto-fluid-mechanic case of a magnetic field applied at an oblique angle with respect to the discontinuity, but under the severe restrictions that both the energy released (or absorbed) and the Alfvén speed is much less than the square of the acoustic velocity. Barmin (1961) performed similar calculations but he relaxed the restrictions imposed upon the magnetic field.

In this study we relax both of the severe restrictions in Demutskii & Polovin's work and consider the flow of a perfectly conducting gas with an orientation in

* Now at the Division of Interdisciplinary Studies and Research, State University of New York, Buffalo.

which the magnetic field is inclined at an arbitrary angle to the normal of the surface of discontinuity.

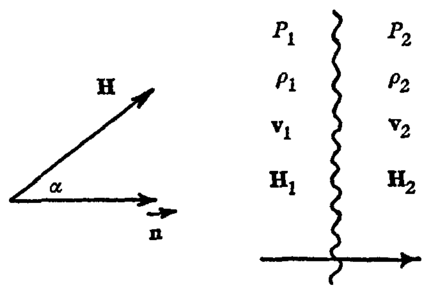

FIGURE 1. The orientation of the flow model.

All variables are considered to be dependent functions only of the co-ordinate normal to the surface and it will be assumed that all gradients vanish at the upstream and downstream conditions.

2. Governing equations

At the surface of the discontinuity, the boundary conditions are that the conservation laws (mass, momentum and energy) are valid and that the tangential electric and normal magnetic fields will be continuous.

These equations may be written in the form:

$$[v_n \rho] = 0 = [m], \tag{1}$$

$$[P + \rho v_n^2 + \tfrac{1}{2}\mu H_t^2] = 0, \tag{2}$$

$$[mv_t - \mu H_n H_t] = 0, \tag{3}$$

$$m[I + \tfrac{1}{2}v_n^2 + \tfrac{1}{2}v_t^2 + \mu H_t^2/\rho - \mu H_n H_t v_t/m] = q, \tag{4}$$

$$[H_n v_t - v_n H_t] = 0, \tag{5}$$

$$[H_n] = 0, \tag{6}$$

where the brackets $[f]$ indicate the jump in the quantity f across the discontinuity, the subscripts n and t respectively refer to the normal and tangential components, I is the enthalpy, q is the heat release and the rest of the symbols have their usual meaning.

In the study of flow discontinuities, it is well known that knowledge of the boundary conditions on the discontinuity is not sufficient to determine uniquely the physical solutions. Thus in ordinary fluid mechanics the boundary conditions include rarefaction shocks as a non-physical solution and it is necessary to supplement these boundary conditions with the additional requirement that the entropy condition be satisfied.

In more complicated systems, such as magnetohydrodynamic discontinuities, rarefaction shocks are also disregarded since they violate the Second Law; however, while the entropy condition is necessary it is no longer sufficient for selecting which compressive shocks are physically relevant from the solutions satisfying the boundary conditions (Jeffery & Taniuti 1964; Akhiezer, Liubarskii & Polovin 1959; Polovin 1961).

The selection principle for obtaining the physically relevant solutions will be, what the literature has termed, the evolutionary condition. It is a stability criterion.

Following Jeffery & Taniuti, this condition may be stated in the following convenient form:

A discontinuity is evolutionary if and only if the number of small amplitude outgoing waves diverging from the discontinuity is equal to the number of independent boundary conditions.

3. Possible modes

Applying the evolutionary condition to the present problem, the possible modes of exothermal waves may be determined. For an exothermal hydromagnetic shock-type discontinuity, the number of independent boundary conditions is one less than the actual boundary conditions, while for a deflagration-type discontinuity the independent and actual boundary conditions are the same. This is because the speed of propagation of a deflagration wave does not depend upon the amplitude of the wave, as it does for a shock-type discontinuity. Hence, in order to be evolutionary, the number of outgoing waves must equal six for a MHD exothermic shock-wave and seven for a MHD deflagration wave.

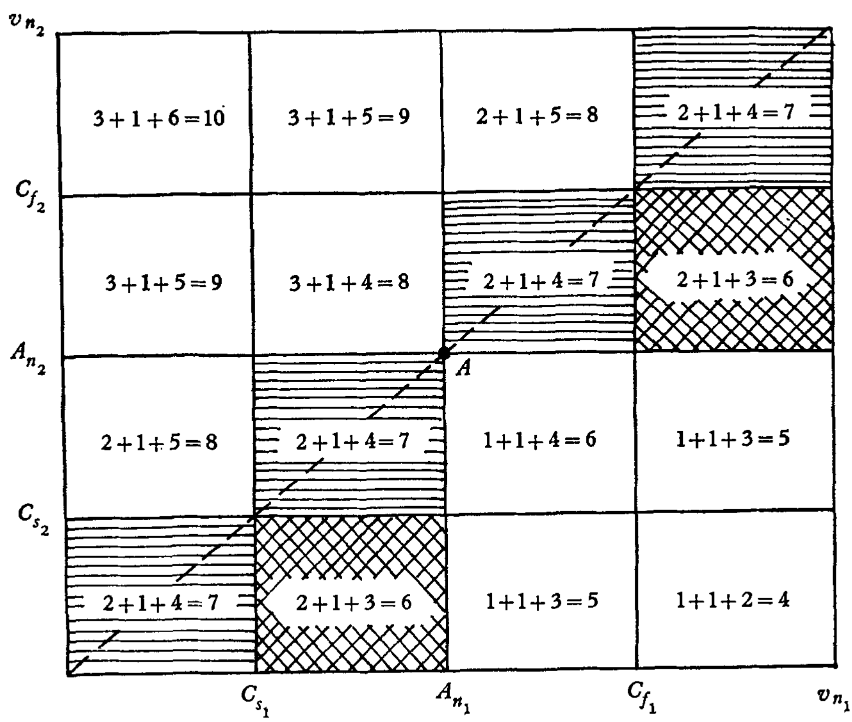

FIGURE 2. The number of diverging waves for the various régimes.

For this flow configuration, there is the possibility of sixteen different régimes resulting from the existence of three velocities of propagation of small disturbances, the Alfvén velocity A and the fast and slow magneto-acoustic velocities C_f, C_s. These quantities may be shown to satisfy the inequality $C_f \geqslant A_n, a \geqslant C_s$, where the equality holds if the transverse component of the magnetic field is zero.

The number of diverging waves for the various régimes were calculated and are shown on the familiar (V_1, V_2)-plane (figure 2). Here the first number equals the number of Alfvén waves, the second equals the number of entropy waves and the third is the total number of fast and slow waves. The dotted line indicates points where the density is continuous, i.e. $v_{n_1} = v_{n_2}$.

At first it appears that there are three possible modes for exothermic shock waves, however, in computing the number of diverging waves it is necessary not only to carry out this procedure for the aggregate of the variables but it must also be performed for any subgroup of these variables. When this is done, the régime $C_{f_1} > v_{n_1} > A_{n_1}, A_{n_2} > v_{n_2} > C_{s_2}$ is no longer found to be evolutionary and is contracted to the point 'A' denoting an Alfvén type discontinuity.

Using figure 2, it is then immediately apparent that in magneto-fluid-mechanics there are two possible modes for exothermic shock waves:

(*a*) Fast exothermic shocks

$$v_{n_1} > C_{f_1}, \quad C_{f_2} > v_{n_2} > A_{n_2}. \tag{7a}$$

(*b*) Slow exothermic shocks

$$A_{n_1} > v_{n_1} > C_{s_1}, \quad C_{s_2} > v_{n_2}. \tag{7b}$$

These are indicated in figure 2 by the cross-hatched shading. In addition, there are four possible modes for MHD deflagration waves:

(*a*) Fast deflagration

$$v_{n_1} > C_{f_1}, \quad v_{n_2} > C_{f_2}. \tag{8a}$$

(*b*) Super-Alfvén deflagration

$$C_{f_1} > v_{n_1} > A_{n_1}, \quad C_{f_2} > v_{n_2} > A_{n_2}. \tag{8b}$$

(*c*) Sub-Alfvén deflagration

$$A_{n_1} > v_{n_1} > C_{s_1}, \quad A_{n_2} > v_{n_2} > C_{s_2}. \tag{8c}$$

(*d*) Slow deflagration

$$C_{s_1} > v_{n_1}, \quad C_{s_2} > v_{n_2}. \tag{8d}$$

The horizontal shading in figure 2 indicates these modes. Finally, there is the possibility of a mode corresponding to the point 'A':

Rotational combustion

$$v_{n_1} = v_{n_2} = A. \tag{9}$$

These are to be contrasted with the single exothermic shock mode (detonation) and the two deflagration modes (subsonic and supersonic combustion) which arise in combustion theory in the absence of magnetic fields.

4. Rotational combustion

Since the rotational combustion mode appears to arise as an exceptional case, it will be considered separately from the rest. From (9) the criterion for this mode is that

$$v_{n_1} = v_{n_2} = A.$$

There are two possible cases by which this criterion may be satisfied: (*a*) $m = 0$, and (*b*) $m \neq 0$, $[\rho] = 0$.

It is immediately apparent that the case $m = 0$ is a trivial solution since there can be no heating at either a contact surface or a tangential discontinuity. The only motion of material is parallel to the discontinuity surface and since there must be an influx of reacting substances for a reaction to exist, this case cannot represent any type of exothermic wave.

However, case (*b*) offers a possible combustion mode unique to MHD. Since the mass flux is continuous, we have

$$m \neq 0, \quad [v_n] = 0, \quad [\rho] = 0. \tag{10}$$

Eliminating $[v_t]$ between (3) and (5) gives

$$v_{n_1} = v_{n_2} = (\mu H_n^2/\rho)^{\frac{1}{2}}, \tag{11}$$

which is the velocity of propagation of this wave. Alternately, eliminating H_n in these equations results in the expression

$$v_{t_2} - v_{t_1} = (\mu/\rho)^{\frac{1}{2}}(T_{t_2} - T_{t_1}). \tag{12}$$

As a consequence of (10), (2) reduces to

$$P_2 - P_1 = -\tfrac{1}{2}\mu(H_{t_2}^2 - H_{t_1}^2). \tag{13}$$

Using the relation $I = U + P/\rho$, the energy equation may be written for this case in the form

$$m[U] + m/\rho[P + \tfrac{1}{2}\mu H_t^2] + \tfrac{1}{2}m[(v_t - (\mu/\rho)^{\frac{1}{2}} H_t)^2] = q. \tag{14}$$

The third term is zero from (12), while the second vanishes due to (13). Then using the perfect-gas relation $U = P/(\gamma - 1)\rho$, (14) becomes

$$(P_2 - P_1) = (\gamma - 1)\rho_1 q/m. \tag{15}$$

Since the downstream conditions of $\mathbf{H}$ and $\mathbf{v}$ are determined from (13), it is seen that the direction of the outgoing quantities $\mathbf{v}_2$, $\mathbf{H}_2$ are indeterminate. This may be interpreted physically to mean that there is a whole family of compatible solutions for $\mathbf{H}_2$, $\mathbf{v}_2$ and they trace out a regular cone about the normal to the discontinuity.

This is very similar to the usual MHD rotational discontinuity in the sense that the magnetic field and velocity may be rotated through an arbitrary angle about the normal; however, in the present case, there are now discontinuities in the pressure and the tangential components of both the flow velocity and the magnetic field due to the heat release. It follows from (15), (13) and (12) that the magnitude of P is increased while the magnitude of both $\mathbf{v}$ and $\mathbf{H}$ are decreased in passing across this wave. For a fixed value of $\mathbf{H}_1$ and $\mathbf{v}_1$, $\mathbf{H}_2$ and $\mathbf{v}_2$ lie on the surface of a circular cone as shown in figure 3; the angle formed by the generatrix of this cone with the normal will always be different from that between the normal and $\mathbf{H}_1$ except for the case $q = 0$, when both angles become equal.

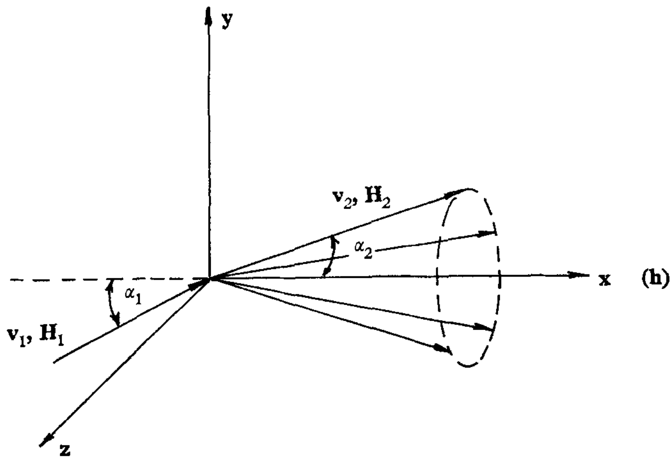

FIGURE 3.

The characteristic property of this mode is that in addition to changing the magnitude of the variables, the fluid may acquire tangential momentum of arbitrary direction on passage through the exothermal discontinuity; therefore the motion is not planar.

Also for a given value of $\mathbf{H}_1$ and $\mathbf{v}_1$, it is seen from (13) and (15) that there is a limit to the allowable heat release corresponding to

$$q = \frac{1}{2}\frac{m\mu H_{t_1}^2}{(\gamma-1)\rho_1}.$$

For q greater than this value, this mode has no physical significance.

5. Oblique combustion modes

Consider now the more interesting type of exothermal discontinuity which is characterized by a discontinuity in both density and normal velocity, i.e.

$$m \neq 0, \quad [\rho] \neq 0, \quad [v_n] \neq 0. \tag{16}$$

For these 'oblique' discontinuities, Friedrichs & Kranzer (1958) have shown that a frame of reference may always be introduced such that the flow velocity $\mathbf{v}$ and the magnetic field $\mathbf{H}$ are parallel on both sides of the discontinuity surface.

It is desired to determine the manner in which the flow variables are altered across these discontinuities. From the tangential-momentum and electric-field equations (3) and (5), the tangential velocity is easily eliminated giving the relation

$$\frac{H_{t_2}}{H_{t_1}} = \frac{m^2/\rho_1 - \mu H_n^2}{m^2/\rho_2 - \mu H_n^2} = \frac{\rho_1(v_{n_1}^2 - A_{n_1}^2)}{\rho_2(v_{n_2}^2 - A_{n_2}^2)}. \tag{17}$$

From the information gained in determining the evolutionary modes for the waves under discussion, it is possible to draw the conclusion that $H_{t_2} \geqslant 0$

(assuming $H_{t_1} \geqslant 0$). This results from the fact that the sign of the quantity $(v_n^2 - A_n^2)$ is the same on either side of the discontinuity for any of the evolutionary modes and noting that $\rho_1/\rho_2 \geqslant 0$. However, it is still impossible to determine whether H_t increases or decreases across the wave since the magnitude of both the denominator and numerator remain unknown. Therefore another expression is required in order to determine the manner of the field variation.

Using the first equality of (17), it is possible, after some algebraic manipulation, to obtain the following expression for the difference between the upstream and downstream magnetic field

$$H_{t_2} - H_{t_1} = \frac{m^2(\rho_2/\rho_1 - 1)\,(H_{t_2} - H_{t_1})}{(v_{n_2}^2 - A_{n_2}^2) + (\rho_1/\rho_2)\,(v_{n_1}^2 - A_{n_1}^2)}. \tag{18}$$

The sign of the denominator is given by the evolutionary conditions for the wave under consideration. Since it is known from (17) that $H_{t_2} \geqslant 0$, it is now possible to determine qualitatively whether H_t increases or decreases once the density ratio is known. For the exothermic shock modes this is easily accomplished. In figure 2 the dotted line gave the locus of points where $\rho_1 = \rho_2$, i.e. $v_{n_1} = v_{n_2}$. Below this line $v_{n_1} > v_{n_2}$ and thus processes occurring in these régimes are compressive. Similarly, above this line, $v_{n_1} < v_{n_2}$ and the processes are of a rarefaction nature.

Therefore, it follows from figure 2 that the two possible modes of MHD exothermic shock waves are compressive in nature. Next, using the inequalities (7*a*) and (7*b*) along with (18) yields the results that the magnetic field increases across a fast exothermic shock wave and decreases across a slow exothermic shock wave.

Unfortunately this method of determining the manner of variation of the magnetic field breaks down for deflagration processes since the information obtainable from figure 2 allows any of the MHD deflagration modes to be compatible with either a compression or rarefaction process.

6. MHD combustion adiabatic

In order to obtain more complete knowledge of the manner in which the dependent variables are altered in these evolutionary modes, the MHD combustion adiabatic was required. Its calculation was most easily performed using a method developed for shocks (Anderson 1963).

Making use of the relations $P = \rho a^2/\gamma$ and $I = a^2/(\gamma - 1)$, the governing equations may be rewritten in the form

$$\rho_1 v_{n_1} = \rho_2 v_{n_2} = m, \tag{1'}$$

$$\rho_1 a_1^2/\gamma + \rho_1 v_{n_1}^2 + \tfrac{1}{2}\mu H_{t_1}^2 = \rho_2 a_2^2/\gamma + \rho_2 v_{n_2}^2 + \tfrac{1}{2}\mu H_{t_2}^2, \tag{2'}$$

$$m v_{t_1} - \mu H_n H_{t_1} = m v_{t_2} - \mu H_n H_{t_2}, \tag{3'}$$

$$a_1^2/(\gamma - 1) + \tfrac{1}{2}v_{n_1}^2 + \tfrac{1}{2}v_{t_1}^2 + (\mu H_{t_1}/m)\,(v_{n_1} H_{t_1} - v_{t_1} H_n) + q$$
$$= a_2^2/(\gamma - 1) + \tfrac{1}{2}v_{n_2}^2 + \tfrac{1}{2}v_{t_2}^2 + (\mu H_{t_2}/m)\,(v_{n_2} H \; - v_t H_n), \tag{4'}$$

$$H_n v_{t_1} - v_{n_1} H_{t_1} = H_n v_{t_2} - v_{n_2} H_{t_2}, \tag{5'}$$

$$H_{n_1} = H_{n_2} = H_n. \tag{6'}$$

Eliminating the tangential velocity from (3′) and (5′) and dividing the result by H_n gives the dimensionless equation for H_t

$$\tan\alpha_2 = \frac{\rho_2(v_{n_1}^2/A_{n_1}^2 - 1)}{\rho_1(v_{n_1}^2/A_{n_1}^2 - \rho_2/\rho_1)}\tan\alpha_1, \tag{19}$$

where α_i is the angle between the magnetic field and normal to the discontinuity.

Alternately, eliminating H_t from (3′) and (5′) yields

$$v_{t_2} = v_{t_1} + (\tan\alpha_1)\frac{(\rho_2/\rho_1 - 1)}{(v_{n_1}^2/A_{n_1}^2 - 1)}. \tag{20}$$

The normal momentum equation (2′) may be made dimensionless by dividing it with H_n^2. Then using (19) to eliminate $\tan\alpha_2$ in the resulting equation yields

$$\frac{1}{\gamma}(\Delta_2 - \Delta_1) - K_1\left(\frac{\eta - 1}{\eta}\right) = \frac{K_1^2(1-\eta^2) - 2K_1(1-\eta)}{2(K_1-\eta)^2}\tan^2\alpha_1, \tag{21}$$

where the following dimensionless group have been used:

$$\eta = \rho_2/\rho_1, \quad K_i = v_{n_i}^2/A_{n_i}^2, \quad \Delta_i = a_i^2/A_{n_i}^2 \quad (i = 1, 2).$$

Next the energy equation is put in dimensionless form on dividing it by the square of the downstream Alfvén velocity $A_{n_2}^2$. After eliminating the tangential velocity and magnetic field components using (19) and (20), we obtain

$$\frac{1}{\gamma - 1}(\Delta_2 - \Delta_1\eta) + \frac{1}{2\eta}K_1(1-\eta^2) + \frac{\eta(\eta-1)K_1(2K_1 - \eta + 1)}{2(K_1-\eta)^2}\tan^2\alpha_1 = \bar{Q}\eta, \tag{23}$$

where $\bar{Q} = q/A_{n_1}$. Eliminating Δ_2 between these two equations results in a cubic equation in K_1 as a function of the parameters η, Δ_1, $\bar{Q}$, γ and α_1,

$$(K_1 - \eta)^2\left(K_1 + \frac{2\Delta_1\eta}{\eta(\gamma-1) - (\gamma+1)} + \frac{2(\gamma-1)\eta^2\bar{Q}}{(\eta-1)\{\eta(\gamma-1) - (\gamma+1)\}}\right) - \left(\frac{\gamma K_1(\gamma-1) - 2\eta K_1}{\eta(\gamma-1) - (\gamma+1)} - \eta^2\right)K_1\tan^2\alpha_1 = 0. \tag{24}$$

This is a general expression for K_1 in terms of an arbitrary heat release and magnetic field. The roots of K_1 are readily obtained and give the velocity with which the wave moves into the cold gas. In (24) it is seen that there are two singularities, corresponding to $\eta = (\gamma+1)/(\gamma-1)$ and $\eta = 1$, which are also familiar singularities in the non-magnetic theory. At both points K_1 must approach infinity. The point $\eta = (\gamma+1)/(\gamma-1)$ corresponds to maximum compression while $\eta = 1$ corresponds to the limiting case of constant volume detonation.

Once K_1 is known as a function of the parameters η, Δ, $\bar{Q}$, γ and α_1, it is then possible to determine the total pressure ratio P_2^*/P_1^*. Equation (2′) is made dimensionless by dividing by H_n^2 giving

$$\frac{P_2^* - P_1^*}{H_n^2} = \frac{m^2}{H_n^2}\left(\frac{1}{\rho_1} - \frac{1}{\rho_2}\right) = K_1\left(1 - \frac{1}{\eta}\right).$$

After expanding the left-hand side of this equation, one obtains

$$\frac{P_2^*}{P_1^*} = 1 + \frac{2\gamma K_1(1-1/\eta)}{2\Delta_1 + \gamma \tan^2\alpha_1}. \tag{25}$$

Substitution of the roots of (24) for K_1, then gives the combustion adiabatic (Hugoniot curve) in the (P^*, τ)-plane. Figure 4 is a sketch of a typical adiabatic. The interesting point of the MHD combustion adiabatic is that it has multiple branches. Additionally it appears that only on one of these branches is it possible to reach large final pressures. This may be substantiated using (24) and noting that in order to reach large final pressures $K_1 \gg \eta$. Then neglecting small terms, (24) reduces to

$$K_1^2\left(K_1 + \frac{2\Delta_1\eta + 2(\gamma-1)\eta^2\bar{Q}/(\eta-1) - [\gamma(\eta-1) - 2\eta]\tan^2\alpha_1}{\eta(\gamma-1) - (\gamma+1)}\right) = 0. \tag{26}$$

Thus it is seen that two of the roots vanish, indicating the existence of only one branch for large final pressures. It is shown in the next section that this upper branch of the curve corresponds to the 'fast' branch.

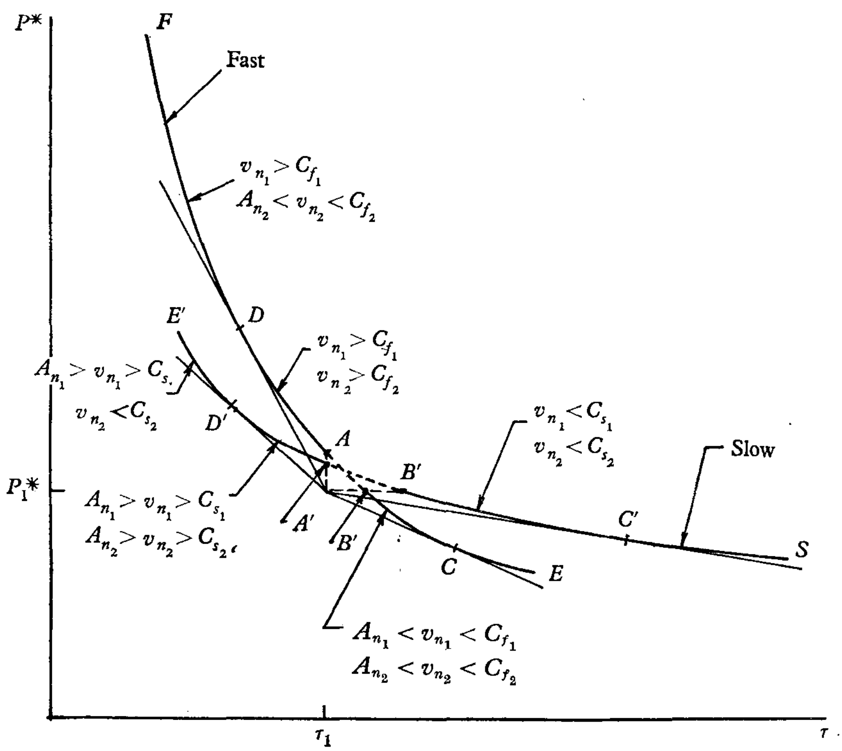

FIGURE 4. The MHD exothermal adiabatic in the (P^*, τ)-plane F–D–A–B–C–E corresponds to the fast branch, E'–D'–A'–B'–C'–S corresponds to the slow branch.

7. Properties of the MHD combustion adiabatic

We now wish to determine some of the properties of this curve. Draw vertical and horizontal lines $1A'A$ and $1BB'$ to the adiabatic. It is easily seen that the portion of the curve lying between either AB or $A'B'$ (dotted) has no physical significance. On this section $P_2^* > P_1^*$, $\tau_2 > \tau_1$, and therefore the expression for the mass flux obtained from (2) $m^2 = [(P_2^* - P_1^*)/(\tau_1 - \tau_2)]$ is imaginary.

Next draw straight lines through the initial point (P_1^*, τ_1) tangent to the Hugoniot. This locates points D, D' and C, C' on the branches of the adiabatic. Hence for each of the points of tangency the following relation is valid

$$\frac{dP^*}{d\tau} = \frac{P_2^* - P_1^*}{\tau_2 - \tau_1}, \tag{27}$$

where $\tau = 1/\rho$, the specific volume.

In the following discussion, it will be convenient to have the Hugoniot expressed in a form different from that used in the previous section. Eliminating the tangential velocity and mass in the governing equations (1) to (6) it follows directly that the Hugoniot function $\psi(P, \tau)$ may be expressed as

$$\psi(P_2, \tau_2) = U(P_2, \tau_2) - U(P_1, \tau_1) + \tfrac{1}{2}(P_2 - P_1)(\tau_2 - \tau_1) + \tfrac{1}{4}(H_{t_2} - H_{t_1})^2(\tau_2 - \tau_1) - q, \tag{28}$$

where state 2 is considered variable. Differentiating (28) and dropping the subscript 2 for the present gives

$$d\psi(P, \tau) = dU(P, \tau) + \tfrac{1}{2}(\tau - \tau_1)\,dP + \tfrac{1}{2}(P - P_1)\,d\tau + \tfrac{1}{2}(H_t - H_{t_1})(\tau - \tau_1)\,dH_t + \tfrac{1}{4}(H_t - H_{t_1})^2\,d\tau.$$

Substituting the thermodynamic relation $dU = TdS - Pd\tau$ into this equation and combining terms results in

$$d\psi(P, \tau) = TdS + \tfrac{1}{2}(\tau - \tau_1)\,dP^* - \tfrac{1}{2}(P^* - P_1^*)\,d\tau + \tfrac{1}{2}(H_t^2 - H_t H_{t_1})\,d\tau - \tfrac{1}{2}(\tau - \tau_1) H_{t_1}\,dH_t. \tag{29}$$

Differentiating equations (2) and (17), substituting the result into (29) and making use of the definition of $\tan\alpha_1$, and K_1, it immediately follows that the Hugoniot function may be expressed in the following useful form:

$$d\psi((P^*, \tau) = TdS + \frac{1}{2}\left(1 + \frac{\tan^2\alpha_1}{(1 - K_1\tau/\tau_1)^2}\right)[(\tau - \tau_1)\,dP^* - (P^* - P_1^*)\,d\tau]. \tag{30}$$

Substituting (27) into this equation it is seen that ψ and S both have an extremum at the same points and by definition of the points of tangency it follows that

$$d\psi = dS = 0.$$

Hence there is a stationary value of entropy at the inflexion point on the Hugoniot curve.

At the points of tangency

$$T\frac{dS}{d\tau} = \frac{1}{2}\left(1 + \frac{\tan^2\alpha_1}{(1 - K_1\tau/\tau_1)^2}\right)\left[(\tau_1 - \tau)\frac{dP^*}{d\tau} + (P^* - P_1^*)\right] = 0. \tag{31}$$

Expanding the differential dP^* as a function of τ and S, substituting this expression into the preceding equation, collecting terms, dividing by $(\tau_1 - \tau)$ and multiplying by τ^2, we obtain

$$\left[2T-(\tau_1-\tau)\left(1+\frac{\tan^2\alpha_1}{(1-K_1\tau/\tau_1)^2}\right)\left(\frac{\partial P^*}{\partial S}\right)_\tau\right]\frac{\tau^2}{(\tau_1-\tau)}\frac{dS}{d\tau}$$
$$=\left(1+\frac{\tan^2\alpha_1}{(1-K_1\tau/\tau_1)^2}\right)\left[\tau^2\left(\frac{\partial P^*}{\partial\tau}\right)_S+\frac{(P^*-P_1^*)}{\tau_1-\tau}\tau^2\right]. \tag{32}$$

At the points of tangency $dS/d\tau = 0$, hence (32) reduces to

$$\tau^2\left(\frac{\partial P}{\partial\tau}\right)_S+\tau^2\left(\frac{\partial(\frac{1}{2}\mu H_t^2)}{\partial\tau}\right)_S+m^2\tau^2 = 0. \tag{33}$$

Using (17) to evaluate the second term and noting that

$$a^2 = -\tau^2\left(\frac{\partial P}{\partial\tau}\right)_S,\quad A_n^2 = \mu H_n^2\tau,\quad A_t^2 = \mu H_t^2\tau,\quad A_t^2+A_n^2 = A^2,$$

this becomes

$$v_{n_2}^4-v_{n_2}^2(a_2^2+A_2^2)+A_{n_2}^2a_2^2 = (v_{n_2}^2-C_{f_2}^2)(v_{n_2}^2-C_{s_2}^2) = 0, \tag{34}$$

which is the familiar equation for the fast and slow magneto-acoustic speeds. Hence at the points of tangency, the burnt gas moves with these speeds. It remains to identify on which branch does which speed occur.

Recalling that the fast and slow speeds obey the inequality $C_f > A_n > C_s$, it then follows that of the four tangency points, the ones determined by the chord (m^2 = const.) with the largest negative slope in the compression and expansion regions correspond to the fast branch. Thus the portion of the curve given by *F–D–A–B–C–E* is the 'fast' branch while that given by *E′–D′–A′–B′–C′–S* is the 'slow' branch. To determine whether the tangency points on each branch correspond to a maximum or minimum value of entropy, differentiate (31) with respect to τ. This gives

$$\frac{d^2S}{d\tau^2}=\frac{1}{2T}\left\{1+\frac{\tan^2\alpha_1}{(1-K_1\tau/\tau_1)^2}\right\}(\tau_1-\tau)\frac{d^2P^*}{d\tau^2}+\frac{1}{2}\left\{1+\frac{\tan^2\alpha_1}{(1-K_1\tau/\tau_1)^2}\right\}\left\{(\tau_1-\tau)\frac{dP^*}{d\tau}\right.$$
$$\left.+(P^*-P_1^*)\right\}\frac{d(1/T)}{d\tau}+\frac{1}{T}\left\{(\tau_1-\tau)\frac{dP^*}{d\tau}-(P^*-P_1^*)\right\}\frac{K_1\tan^2\alpha_1}{\tau_1(1-K_1\tau/\tau_1)^3}.$$

Since $dT/d\tau$ and $(K_1/\tau_1)\tan^2\alpha_1(1-K_1\tau/\tau_1)^3$ both remain finite (the second expression becomes infinite at $\tau-\tau_1$, but this point has already been excluded from the present discussion) and the quantity

$$(\tau_1-\tau)\frac{dP^*}{d\tau}+(P^*-P_1^*) = 0,$$

the above expression reduces to

$$\frac{d^2S}{d\tau^2}=\frac{1}{2T}\left(1+\frac{\tan^2\alpha_1}{(1-K_1\tau/\tau)^2}\right)(\tau_1-\tau)\frac{d^2P^*}{d\tau^2}.$$

Now, provided $d^2P^*/d\tau^2 > 0$, we obtain the following:

$\tau_2 < \tau_1$, $d^2S/d\tau^2 > 0$, i.e. a minimum at *D* and *D′*.

$\tau_2 > \tau_1$, $d^2S/d\tau^2 < 0$, i.e. a maximum at *C* and *C′*.

Hence on a given branch of the Hugoniot above $D(D')$ and below $C(C')$ we have $dS_2/d\tau_2 < 0$ while between these points $dS_2/d\tau_2 > 0$.

It remains to prove that $d^2P^*/d\tau^2 > 0$. Along a given branch, a chord (m^2 = const.) drawn through P_1^*, τ_1 with a negative slope slightly greater than the tangent condition at $D(D')$ intersects the branch in two places. This implies a minimum at the point of tangency, i.e. $d^2P^*/d\tau^2 > 0$. In a similar manner this may also be shown for $C(C')$. Once it is known how $dS/d\tau$ varies, it follows immediately from (32) that for $\tau < \tau_1$, $v_{n_2} < C_{i_2}$ above the tangency point $D(D')$ and $v_{n_2} > C_{i_2}$ below it, while for $\tau > \tau_1$, $v_{n_2} > C_{i_2}$ beyond the tangency point $C(C')$ and $v_{n_2} < C_{i_2}$ to the left of it. Here C_i refers to either C_f or C_s depending on which branch is being considered.

Finally, the upstream velocity for the various portions of the curve may be determined from a simple graphical argument. The velocity of sound in the unburnt gas is given by the slope of the tangent to the shock adiabatic while v_{n_1} is given by the chord (m^2 = const.). Since all of the chords are steeper than their corresponding tangents to the shock adiabatic, for $\tau < \tau_1$ we obtain $v_{n_1} > C_{f_1}$ and $v_{n_1} > C_{s_1}$ on their respective branches. In a similar manner for $\tau > \tau_1$ we get $v_{n_1} < C_{f_1}$, $v_{n_1} < C_{s_1}$ on their respective branches. Since it is now known how P^*/P_1^* and ρ_1/ρ_2 vary for each of the evolutionary modes, the manner in which the magnetic field changes may be determined using (18). Additionally knowing how ρ_2/ρ_1 varies allows the manner of variation in the gas pressure P_2/P_1 to be resolved.

From figure 4 it is known that the density and total pressure increases in fast and sub-Alfvén deflagration and decreases in super-Alfvén and slow deflagration. Hence the magnetic field increases across a fast and slow deflagration and decreases across a super- and sub-Alfvén deflagration. From the foregoing it then follows that the gas pressure increases in fast and sub-Alfvén deflagration, decreases in slow deflagration and may do either in the super-Alfvén mode.

The manner of variation of the dependent variables for a MHD exothermic shock wave was previously determined utilizing figure 2.

8. Discussion

A general expression for an arbitrary magnetic field and heat release was derived for the MHD combustion adiabatic. The resulting curve was third order and gave rise to two separate evolutionary branches, a 'fast' and 'slow' branch. Along these two branches, the evolutionary combustion modes consisting of two MHD exothermic shock régimes and four deflagration régimes were located. It was found that the tangents to each of these branches corresponded to having the burnt gases moving with the 'fast' and 'slow' magneto-acoustic speeds. On the compression portions of these two branches, the points, of tangency were found to be points of minimum entropy, while on the rarefaction portions the tangency points corresponded to points of maximum entropy.

From the adiabatic it was seen that both the density and the total pressure increased in fast and sub-Alfvén deflagration modes and decreased in super-Alfvén and slow deflagration modes. Additionally, it was learned that the magnetic field increases across the fast and slow deflagration wave and decreases across the super- and sub-Alfvén deflagration waves. For the two MHD exothermic shock modes, the total pressure and density increases upon passing through the waves while the magnetic field increases across the fast detonation wave and decreases across the slow detonation mode. It appeared from studying the roots of the combustion adiabatic that only the fast branch exists for large pressures.

The other combustion mode studied in this investigation was rotational combustion. This unique MHD combustion mode exists with no change in density across the wave and has the unusual feature that the gas mass acquires tangential momentum of arbitrary direction on passage through this discontinuity while undergoing a jump in the magnitude of the velocity and magnetic field.

The author is indebted to Prof. Ali Bulent Cambel for suggesting this problem and to the Northwestern University Computing Center for providing computation services.

REFERENCES

AKHIEZER, A. I., LIUBARSKII, G. Ia. & POLOVIN, R. V. 1959 *Sov. Phys. JETP*, **8**, 507.

ANDERSON, J. E. 1963 *Magnetohydrodynamic Shock Waves*. Cambridge: M.I.T. Press.

BARMIN, A. A. 1961 *Sov. Phys. Doklady*, **6**, 374.

DEMUTSKII, V. P. & POLOVIN, R. V. 1961 *Sov. Phys. Tech. Phys.* **6**, 302.

FONG, M. C., BOLLINGER, L. E. & EDSE, R. 1961 *Wright-Patterson ARL Rep.* no. 69.

FRIEDRICHS, K. O. & KRANZER, H. 1958 *New York Univ. Rep.* NYO-6486-VIII.

GROSS, R. A., CHINITZ, W. & RIVLIN, R. J. 1960 *J. Aero/Space Sci.* **27**, 283.

HELLIWELL, J. B. 1962 *J. Fluid Mech.* **14**, 405.

JEFFERY, A. & TANIUTI, T. 1964 *Non-Linear Wave Propagation with Applications to Physics and Magnetohydrodynamics*. New York: Academic Press.

LARISH, E. & SHEKHTMANN, I. 1958 *Sov. Phys. JETP*, **18**, 1.

LYUBIMOV, G. A. 1959 *Sov. Phys. Doklady*, **4**, 526.

POLOVIN, R. V. 1961 *Sov. Phys. Uspekhi*, **3**, 5.